Modelling the migration of contaminants through variably saturated dual-porosity, dual-permeability chalk

Manuscript accepted for publication in the Journal of Contaminant Hydrology

September 2005

Serge Brouyère

Hydrogeology Group, Department of Georesources, Geotechnologies and Building Materials (GEOMAC) and Aquapôle

Building B52/3, University of Liège

B-4000 Sart Tilman

Belgium

Tel: +32-43662377

Fax: +32-43669520

E-Mail: Serge.Brouyere@ulg.ac.be

Abstract

In the Hesbaye region in Belgium, tracer tests performed in variably saturated fissured chalk rocks presented very contrasting results in terms of transit times, according to artificially controlled water recharge conditions prevailing during the experiments. Under intense recharge conditions, tracers migrated across the partially or fully saturated fissure network, at high velocity in accordance with the high hydraulic conductivity and low effective porosity (fracture porosity). At the same time, a portion of the tracer was temporarily retarded in the almost immobile water located in the matrix. Under natural infiltration conditions, the fissure network remained inactive. Tracers migrated downward through the matrix, at low velocity in relation with the low hydraulic conductivity and the large porosity of the matrix. Based on these observations, Brouyère et al. (2004a) proposed a conceptual model in order to explain the migration of solutes in variably saturated, dual-porosity, dual-permeability chalk. Here, mathematical and numerical modelling of tracer and contaminant migration in variably saturated fissured chalk is presented, considering the aforementioned conceptual model. A new mathematical formulation is proposed to represent the unsaturated properties of the fissured chalk in a more dynamic and appropriate way. At the same time, the rock water content is partitioned between mobile and immobile water phases, as a function of the water saturation of the chalk rock. The groundwater flow and contaminant transport in the variably saturated chalk is solved using the control volume finite element method. Modelling the field tracer experiments performed in the variably saturated chalk shows the adequacy and usefulness of the new conceptual, mathematical and numerical model.

Keywords: dual-porosity, dual-permeability, fissured chalk, transport model, unsaturated zone, retention curve, relative hydraulic conductivity

Introduction

Recently, Brouyère et al. (2004a) have presented the results of an experimental study performed in the Hesbaye region in Belgium in order to characterize and to quantify hydrodynamic and hydrodispersive processes governing the downward migration of solute contaminants (e.g., nitrates) across the unsaturated zone overlying a fissured chalk aquifer. One of the most significant observations drawn from these experiments is the high contrast in terms of tracer transit times across the unsaturated chalk depending on the application of an artificial water recharge (forced gradient conditions) in the injection well or not (natural infiltration conditions). Tracer transit times across the unsaturated zone varied from a few hours when forced gradient conditions prevailed to almost one year under natural infiltration conditions.

The tracer test results can be explained by the dual-porosity, dual-permeability of the chalk. In the fissured chalk, groundwater flow and transport conditions can be highly variable according to the degree of water saturation of the rock. Under normal recharge conditions, fissures remain empty in the unsaturated zone of the chalk and a slow regime of flow and contaminant transport is active in the matrix characterised by a low hydraulic conductivity and a high porosity. In the saturated zone, or under intensive recharge conditions in the unsaturated zone, water and contaminants migrate at high velocity along the partially or fully saturated fissures controlling the hydraulic conductivity of the rock mass. The effective porosity is low, representing the contribution of fissures to the total porosity of the chalk. At the same time, transported contaminants are subject to retardation in the matrix (matrix diffusion) where the water can be considered as immobile compared to the water moving in the fissure network. The transport mechanism across the fissured chalk is schematised in Figure 1.

This conceptualisation of the dynamic behaviour of chalk hydraulic and hydrodispersive properties explained, from a conceptual point of view, the tracer test results (Brouyère et al. 2004a). However, a transcription into a mathematical model was required. Below, the mathematical model developed in order to represent more accurately the variations in hydraulic conductivity and effective porosity of the chalk with respect to infiltration conditions and degree of saturation of the chalk is presented. The numerical solution of groundwater flow and contaminant transport in the variably saturated chalk, using the three-dimensional finite element simulator SUFT3D is described. Modelling results of the field tracer experiments performed in the chalk, used to illustrate the developments, support the conceptual model and demonstrate that the mathematical model is adequate to explain the tracer experiments.

1 Modelling the hydraulic and hydrodispersive behaviour of the variably saturated chalk

Many conceptual and mathematical models were proposed to simulate the hydrodynamic behaviour of structured media characterised by preferential flow paths such as fissured rocks or aggregate soils (e.g., Bai et al. 1993, Pruess et al. 1999, Berkowitz 2002). Most advanced concepts rely on a distinct modelling of the preferential flows paths and the matrix (e.g., Gwo 1992, Dykhuizen 1987, 1990, VanderKwaak 1999). Such approaches are relatively complicated and they require a large number of parameters that are often not available for characterizing both hydraulic networks and their interactions. Consequently, they are frequently not suitable for practical (field scale) applications. Another solution is to consider the medium as a single continuum (e.g., Peters and Klavetter 1988, Berkowitz et al. 1988, Finsterle 2000) by assuming a pressure equilibrium between the matrix and the fissures. In that case, the mathematical relationships used to model the hydraulic behaviour of the rock

mass under variably saturated conditions have to be adapted to account for the dynamic evolution of flow conditions according to the degree of saturation of the rock. Two characteristic curves need to be defined: the retention curve $\theta(h)$ linking the water content θ (dimensionless) to the applied suction head h (L), and the hydraulic conductivity curve $k_r(\theta)$ relating the evolution of the relative hydraulic conductivity k_r (dimensionless) with the water content θ. Classical mathematical relationships used to model unsaturated properties (e.g. van Genuchten 1980, Mualem 1976) are not directly suited as they do not allow an accurate representation of the unsaturated behaviour of the underground medium close to saturation. These relationships implicitly rely on a uni-modal distribution of pore dimensions (Fredlung and Xing 1994). In structured media, such as in fissured chalk, this distribution is at least bi-modal, often multi-modal (Price et al. 1993, Younger and Elliot 1995). Several relationships, based on bi- or multi-modal distributions of pore space, were proposed in the literature for modelling the unsaturated properties of structured media (e.g., Smettem and Kirby 1990, Othmer et al. 1991, Ross and Smettem 1993, Durner 1994, Fredlung and Xing 1994, Fredlung et al. 1994, Mallants et al. 1997). However, these models, usually developed for representing the retention curve, do not allow an analytical derivation of the relationship between the hydraulic conductivity and the water content from the retention curve. Furthermore, they are usually not continuously derivable, a condition that is not essential but interesting if groundwater flow simulations require the computation of derivatives of the unsaturated characteristic curves, such as Newton linearization (e.g., Paniconi et al. 1991, Paniconi and Putti 1994). The new mathematical relationships proposed here after to model the unsaturated characteristic curves of the chalk overcome these problems and they still offer a relatively large flexibility for modelling the unsaturated properties of structured media.

1.1 Retention curve

For modelling the unsaturated properties of fissures, a model such as that of Wang and Narasimhan (1985) could probably be very suited. However, it requires a detailed knowledge of the morphology and distribution of fissures, which is not available here. The retention curve of the chalk is modelled here using the combination of two van Genuchten relationships, one defined for the matrix, one for the fissures.

Up to this point, the model used for the retention curve is similar to that of Ross and Smettem (1993) or Durner (1994). In contrast to these models that just sum the two retention curves to build the global functionality describing the retention curve of the structured medium, the approach proposed here forces a continuously derivable transition between the relations that describe the matrix and the fissure component respectively (Figure 2). Accordingly, it is possible to derive analytically the hydraulic conductivity curve from the retention curve across the whole range of water contents.

The relationship used to model the retention curve associated with the matrix is (Figure 2, light grey curve):

$$\Theta_M = \frac{\theta - \theta_r}{\theta_{s,M} - \theta_r} = \left[1 + \left(\alpha_M h\right)^{n_M}\right]^{-m_M} \qquad (1)$$

where θ_r is the residual water content of the matrix; $\theta_{s,M}$ (dimensionless), to be considered just as a fitting parameter, is the 'equivalent' saturated water content of the matrix, close but different from the matrix total porosity n_m (dimensionless); α_M (L^{-1}), n_M (dimensionless) and m_M (dimensionless) are the van Genuchten parameters used to fit the portion of the retention curve associated with the matrix; Θ_M (dimensionless) is the relative saturation of the matrix.

The relationship used to model the retention curve associated with the fissure component of the chalk is (Figure 2, dark grey curve):

$$\Theta_F = \frac{\theta - \theta_{r,F}}{\theta_s - \theta_{r,F}} = \left[1 + (\alpha_F h)^{n_F}\right]^{-m_F} \quad (2)$$

where $\theta_{r,F}$ (dimensionless), to be considered just as a fitting parameter, is the 'equivalent' residual water content of the fissure; θ_s (dimensionless) is the saturated water content of the chalk rock; α_F (L^{-1}), n_F (dimensionless) and m_F (dimensionless) are the van Genuchten parameters used to fit the portion of the retention curve associated with the fissures; Θ_F (dimensionless) is the relative saturation of the fissures.

At the point (θ_J, h_J) common to the matrix and fissure retention curves (Figure 2), continuity conditions can be expressed as follows:

-continuity of the retention curve: $(\theta_J, h_J)_M = (\theta_J, h_J)_F$ (3a)

-continuity of the first derivative of the retention curve: $\left(\frac{\partial\theta}{\partial h}\right)_{J,M} = \left(\frac{\partial\theta}{\partial h}\right)_{J,F}$ (3b)

This comes to solving the following equation system in terms of $\theta_{r,F}$ and n_F (Brouyère 2001):

$$\chi(\theta_{r,F}, n_F) = \theta_{r,F} - \frac{\theta_r + (\theta_{s,M} - \theta_r)\left(1 + (\alpha_M h_J)^{n_M}\right)^{-m_M} + \theta_s\left(1 + (\alpha_F h_J)^{n_F}\right)^{-m_F}}{\left(1 + \left(1 + (\alpha_F h_J)^{n_F}\right)^{-m_F}\right)} = 0 \quad (4a)$$

$$\gamma(\theta_{r,F}, n_F) =$$
$$-\frac{\alpha_M m_M (\theta_{s,M} - \theta_r)}{1 - m_M}\Theta_{J,M}^{1/m_M}\left(1 - \Theta_{J,M}^{1/m_M}\right)^{m_M} + \frac{\alpha_F m_F (\theta_s - \theta_{r,F})}{1 - m_F}\Theta_{J,F}^{1/m_F}\left(1 - \Theta_{J,F}^{1/m_F}\right)^{m_F} = 0 \quad (4b)$$

In practice, the adjustment of the retention curve representative of the chalk rock is performed as follows. First, the porosities associated with the matrix and the fissures respectively are defined, the total of these two values being set equal to the saturated water content θ_s of the rock. The van Genuchten parameters relative to the matrix (α_M, n_M and $\theta_{s,M}$) are obtained by fitting Equation (1) on retention curves measured on chalk matrix samples (see Brouyère et

al. 2004a). An estimation has to be provided for the capillary rise ($\psi_F = 1/\alpha_F$) in the fissure network. Estimates of the capillary rise in the fractures can be found in the literature (e.g., Price et al. 1993). The parameters n_F and $\theta_{r,F}$ are determined by solving the equation system (4a) and (4b) in order to meet the conditions (3a) and (3b).

1.2 Relative hydraulic conductivity curve

In order to derive the relationship between the hydraulic conductivity and the water content analytically from the retention curve, the model of Mualem (1976) is considered. This model was used already for the estimation of the evolution of hydraulic conductivity in fissured rocks (Peters and Klavetter 1988). The fundamental relationship of Mualem's model is:

$$k_r(\theta) = S_e^P \left[\frac{f(\theta)}{f(\theta_s)} \right]^2 = S_e^P \left[\frac{\int_0^{\theta} d\theta / h}{\int_0^{\theta_s} d\theta / h} \right]^2 \tag{5}$$

In Equation (5), P is a parameter for which an optimal value of 0.5 was proposed and $S_e = \frac{\theta - \theta_r}{\theta_s - \theta_r}$.

When the matrix is partially saturated and the fissures are completely desaturated, mathematical integration is performed along the retention curve describing the matrix (Equation 1):

$$f_M(\theta) = \int_{\theta_r}^{\theta} \frac{d\theta}{h} = \alpha_M (\theta_{s,M} - \theta_r) \left(1 - \left(1 - \Theta_M^{1/m_M} \right)^{m_M} \right) \tag{6a}$$

For a fully saturated matrix and partially saturated fissures, integration starts from $\theta = \theta_J$ and it is performed along the retention curve describing the fissures (Equation 2):

$$f(\theta) = f_M(\theta_J) + f_F(\theta) \tag{6b}$$

1 with $f_F(\theta) = \int_{\theta_J}^{\theta} \frac{d\theta}{h} = \alpha_F (\theta_s - \theta_{r,F}) \left[\left(1 - \Theta_{J,F}^{1/m_F} \right)^{m_F} - \left(1 - \Theta_F^{1/m_F} \right)^{m_F} \right]$ (6c)

2 $\Theta_{J,F} = \frac{\theta_J - \theta_{r,F}}{\theta_s - \theta_{r,F}}$

3 The evaluation of Equation (6c) in $\theta = \theta_S$ gives:

4 $f(\theta_s) = f_M(\theta_J) + f_F(\theta_s)$ (6d)

5 Introducing Equations (6b) and (6d) into Equation (5) provides the functionality to describe
6 the evolution of the relative hydraulic conductivity with the water content $k_r(\theta)$. For
7 completeness, Annex 1 provides the mathematical expressions for the derivatives $d\theta/dh$ and
8 dk_r/dh, needed for numerical solution of the Richards equation using Newton-Raphson
9 linearization.

10 Figure 3 shows the characteristic curves obtained using mean van Genuchten parameters
11 estimated by fitting the retention curves measured on the chalk matrix samples and using
12 literature values for the fissure characteristics (Brouyère 2001, Brouyère et al. 2004a). The
13 relative hydraulic conductivity curve shows the expected evolution with water content or
14 suction head. For a small suction applied, fissures desaturate and the hydraulic conductivity of
15 the chalk rock drops by several orders of magnitude. Afterwards, the water content and the
16 relative hydraulic conductivity show a slower variation when the suction is increased. The
17 relationship reproduces the strong reduction in hydraulic conductivity observed when the
18 fissure network is inactive (here, a reduction by a factor 100). This validates a posteriori the
19 use of Mualem's model together with the proposed bi-modal retention curve.

20 The way the two retention curves are combined to create the global retention curve means that
21 until the matrix is fully saturated, fissures are empty and remain inactive. This implies that the
22 retention model cannot accommodate by-pass flows observed when there is pressure
23 disequilibrium between the fissures and the matrix. Therefore, the use of the model is

restricted to relatively slowly changing infiltration conditions. In the Hesbaye aquifer, the existence of a thick layer of loess smoothes the temporal variations of groundwater recharge rate at the top of the unsaturated chalk layer and the assumption of pressure equilibrium between the matrix and the fissures is likely to occur in the unsaturated zone (Brouyère et al. 2004a). These relationships could also be used to model situations for which fast flow along fissures is observed in the unsaturated zone without pressure disequilibrium, such as water film flows (Tokunaga and Wan 1997, 1998, Tokunaga et al. 2000, Or and Tuller 2000) or fracture surface-zone flows (Tokunaga and Wan 2001). Finally, if pressure disequilibrium and by-pass flow occur, the model proposed here provides a good first approximation.

1.3 Partitioning the chalk porosity according to the water saturation degree

Structured geological formations are often characterized by the presence of an important quantity of immobile or less mobile water located in small pores or in less pervious layers (Gerke and van Genuchten 1993). To compute contaminant transport and retardation in such formations, the dual-porosity, first-order transfer model (Coats and Smith 1964, van Genuchten and Wierenga 1976, Brouyère et al. 2000) introduces two parameters in the calibration process: the immobile water porosity θ_{im} (dimensionlesss) and the first order transfer coefficient α (T^{-1}). The original form of the dual porosity model assumes that the porosity associated with the immobile water is constant. This model will be further called the "classical dual porosity model" (CDPM approach). However, when modelling transient unsaturated groundwater flows, any reduction of water content should affect the distribution of water between mobile and immobile water phases. If one of these terms is assumed constant, for example the immobile water content, when the total water content is reduced by amplitude close to that of the effective porosity, i.e. the mobile water porosity θ_m (dimensionless), the latter tends towards zero, which is physically and mathematically unacceptable (Zurmühl and Durner 1996). In reality, as discussed by Brouyère et al. (2004a),

under variably saturated flow conditions, when the rock mass desaturates, fissures desaturate first and the hydraulic conductivity of the rock mass is globally reduced. In such conditions, water located in the matrix cannot be considered as immobile anymore and it becomes the only vector of mobility of contaminants. In other words, matrix porosity becomes associated with the effective porosity.

It appears that, in order to be applicable in transient variably saturated groundwater flow conditions, the dual porosity first order transfer model has to be adjusted. Water needs to be distributed between mobile and immobile phases, depending of the degree of saturation. Zurmülh and Durner (1996) suggested several criteria, the simplest being the consideration of a constant ratio between the immobile water porosity and the total water content:

$$c_{part} = \frac{\theta_{im}}{\theta} \tag{7a}$$

They also suggested distributing the water according to the ratio of relative hydraulic conductivity values associated with the immobile water and the total water content:

$$c_{part} = \frac{k_r(\theta_{im})}{k_r(\theta)} \tag{7b}$$

With this approach, the hydraulic conductivity curve reflects the distribution of velocities in the medium, analogous to a capillary bundle model (Rao et al. 1976, Toride et al. 1995). This adjusted model will be further called the “dynamic dual porosity model” (DDPM approach). Figure 4 illustrates this concept, using the hydraulic conductivity curve defined for the chalk in the previous section, with a partitioning coefficient c_{part} = 0.01. At saturation, the effective porosity of the chalk rock is small, associated with the fissures, and the quantity of immobile water in the dual porosity is high, associated with the chalk matrix (Figure 4a). When fissures desaturate, the effective porosity of the chalk is higher, associated with a part of the water moving in the matrix. At the same time, the quantity of water that is considered as immobile is reduced (Figure 4b).

1.4 First conclusions

In the variably saturated dual-porosity, dual-permeability chalk, the hydraulic conductivity is likely to change rapidly by several orders of magnitudes and the distribution of water content between mobile and immobile water needs to be continuously updated. The mathematical model presented here above meets these two essential criteria. When the fissures are partially or fully saturated, the model predicts a high hydraulic conductivity and a low effective porosity of the chalk rock. At the same time, dual-porosity effects are likely to be important because of the large porosity of the matrix. When the saturation degree is reduced, fissures become inactive and the hydraulic conductivity curve is reduced by several orders of magnitude. The effective porosity of the chalk rock becomes larger, associated with water present in the rock matrix. The next section describes the adaptations to groundwater flow and contaminant transport equations solved in the SUFT3D code (Brouyère 2001, 2003) for the integration of these concepts.

2 Numerical modelling of groundwater flow and contaminant transport in the variably saturated chalk

2.1 Variably saturated groundwater flow modelling

In the finite element simulator SUFT3D, a generalized form of Richard's equation is used to model groundwater flow in variably saturated conditions:

$$F\frac{\partial h}{\partial t} = \underline{\nabla}\cdot\left[\left(\underline{\underline{K}}_S k_r(\theta)\right)\cdot\underline{\nabla}(h+z)\right] + q \qquad (8)$$

where h is the pressure head (L), positive in the saturated zone and negative in the unsaturated zone; z is the elevation head (L); $\underline{\underline{K}}_S$ is the saturated hydraulic conductivity tensor (L T^{-1}); $k_r(\theta)$ is the relative hydraulic conductivity (-); q is a source/sink term (T^{-1}); and F is a generalized storage coefficient (L^{-1}) that can be expressed as:

$$F = S_s + \frac{d\theta}{dh} \tag{9}$$

In Equation (9), the first term is the specific storage coefficient S_s (L^{-1}) that accounts for the compressibility of water and porous medium. The second term represents the storage of water in the unsaturated zone; it is the first derivative of the retention curve $\theta(h)$ (see Annex 1 for its complete mathematical expression).

In the saturated zone, one can generally consider that the water content is constant ($\theta = \theta_s = \text{constant}$), in which case:

$$\frac{d\theta}{dh} = 0 \tag{10a}$$

In the unsaturated zone, the specific storage coefficient can often be disregarded compared to the water storage term ($S_s << d\theta/dh$), in which case, one can write:

$$F \frac{\partial h}{\partial t} = \frac{d\theta}{dh}\frac{\partial h}{\partial t} = \frac{\partial \theta}{\partial t} \tag{10b}$$

Based on these assumptions, Equation (8) can be expressed as follows:

$$S_s \frac{\partial h}{\partial t} + \frac{\partial \theta}{\partial t} = \underline{\nabla} \cdot \left[\left(\underline{\underline{K_S}} k_r(\theta)\right) \cdot \underline{\nabla}(h + z)\right] + q = \underline{\nabla} \cdot \underline{v}_D + q \tag{11}$$

The term $\underline{v}_D$ in the right-hand side of Equation (11) is the Darcy flux (LT^{-1}). The retention curve $\theta(h)$ and the hydraulic conductivity curve $k_r(\theta)$ are presented in the previous sections. One of the two components of the storage term (left-hand side of Equation 11) is equal to zero depending on whether the computation is performed in the saturated zone or in the unsaturated zone. This formulation, which distinguishes the saturated and the unsaturated parts of the aquifer, is necessary to avoid numerical problems when applying the numerical solution proposed by Celia et al. (1990) which, in its original form, is not suitable to simulate a fully saturated medium.

For unsaturated groundwater flow, the SUFT3D code applies the formulation of Celia et al. (1990) to Equation (11) linearised using Picard, Newton-Raphson or a mixed form of these two schemes (Putti and Paniconi 1992). The numerical solution of Equation (11) is obtained by applying the control volume finite element method (e.g., Letniowski and Forsyth 1991, Therrien and Sudicky 1996). Convergence improvement is achieved using a dynamic relaxation scheme (Cooley 1983) together with the target-based full Newton time stepping scheme proposed by Diersch and Perrochet (1999). The solution to the discretized and linearized equation system is obtained using the sparse-system equation solver WatSolv (VanderKwaak et al. 1997). Details can be found in Brouyère (2001).

2.2 Solute transport modelling

In the SUFT3D code, the general mass conservation equation applied to the solute contaminant in the variably saturated chalk is:

$$\frac{\partial(\theta_m C)}{\partial t} + \frac{\partial(\theta_{im} C_{im})}{\partial t} = -\underline{\nabla} \cdot (\underline{v}_D C) + \underline{\nabla} \cdot (\theta_m \underline{\underline{D}}_h \cdot \underline{\nabla} C) - \lambda(\theta_m C + \theta_{im} C_{im}) + qC' \qquad (12)$$

In Equation (12), the left-hand side represents the storage of solute at a concentrations C (ML^{-3}) in the mobile water (associated porosity θ_m) and C_{im} (ML^{-3}) in the immobile water and (associated porosity θ_{im}). In the right-hand side, the first term is the advective flux. The second term is the hydrodispersive flux ($\underline{\underline{D}}_h$ is the hydrodynamic dispersion tensor, L^2T^{-1}). The third term represents solute degradation in the mobile and the immobile water (λ is the first-order degradation constant, T^{-1}) and the last term accounts for a source/sink, at a rate q (T^{-1}) and concentration C' (ML^{-3}), with $C' = C_{inj}$ if $q > 0$ and $C' = C$ if $q < 0$ (C_{inj} being the concentration in the injected fluid).

Equation (12) is called the divergence form of the transport equation (Diersch 2001, Saaltink et al. 2004). Expanding the mass storage and the advective flux terms in Equation (12) and using Equation (11) gives the advective form of the transport equation:

$$\theta_m \frac{\partial C}{\partial t} + \frac{\partial(\theta_{im} C_{im})}{\partial t} = -\underline{v}_D \cdot \underline{\nabla} C + \underline{\nabla} \cdot (\theta_m \underline{\underline{D}}_h \cdot \underline{\nabla} C) + q(C' - C) - \lambda(\theta_m C + \theta_{im} C_{im}) + \left(F \frac{\partial h}{\partial t} - \frac{\partial \theta_m}{\partial t} \right) C \quad (13)$$

The advective formulation offers several advantages, e.g., when solving chemical reaction problems (Huyakorn et al. 1985) or when applying lagrangian methods to solve advection-dominated problems (Yeh 1990). It has also the advantage of facilitating the implementation of the porosity-partitioning concept.

Mass conservation equation applied to the immobile water alone can be written as:

$$\frac{\partial(\theta_{im} C_{im})}{\partial t} = \alpha(C - C_{im}) - \lambda \theta_{im} C_{im} + f_{\Delta\theta}^{C} \quad (14)$$

In Equation (14), α is the first-order transfer coefficient (T^{-1}) that accounts for diffusive solute exchange between mobile and immobile water, $f_{\Delta\theta}^{C}$ represents solute exchange due to water transfer between mobile and immobile water when the degree of saturation varies with time ('advective' exchange).

Practically speaking, the computation is performed as follows. The groundwater flow simulation is performed on a time step Δt. Based on the results, the variation in water content is evaluated at each calculation point between time t and $t + \Delta t$. At a given calculation point, if the water content θ increases, the immobile water porosity θ_{im} increases proportionally (see Figure 4). In that case, a quantity of water containing solute at a concentration C is "transferred" from the mobile water to the immobile water:

If $\frac{\partial \theta_{im}}{\partial t} > 0$, $f_{\Delta\theta}^{C} = \frac{\partial \theta_{im}}{\partial t} C \approx \frac{\theta_{im}(t + \Delta t) - \theta_{im}(t)}{\Delta t} C = \frac{\Delta \theta_{im}}{\Delta t} C$ (15a)

In contrast, if the water content θ decreases, the immobile water porosity θ_{im} decreases proportionally and a quantity of water containing solute at a concentration C_{im} is transferred from the immobile to the mobile water:

If $\frac{\partial \theta_{im}}{\partial t} < 0$, $f_{\Delta\theta}^{C} = \frac{\partial \theta_{im}}{\partial t} C_{im} \approx \frac{\theta_{im}(t+\Delta t) - \theta_{im}(t)}{\Delta t} C_{im} = \frac{\Delta \theta_{im}}{\Delta t} C_{im}$ (15b)

Considering Equations (15a) and (15b), Equation (14) can be written in a general form:

$$\theta_{im} \frac{\partial C_{im}}{\partial t} = \alpha(C - C_{im}) - \lambda \theta_{im} C_{im} + (C^{*} - C_{im}) \frac{\Delta \theta_{im}}{\Delta t} \quad (16)$$

with $C^{*} = C$ if $\frac{\Delta \theta_{im}}{\Delta t} > 0$

$C^{*} = C_{im}$ if $\frac{\Delta \theta_{im}}{\Delta t} < 0$

In Equation (16), the last term of the right-hand side is only present if the transfer of water occurs from the mobile water to the immobile water.

Introducing Equation (16) into Equation (13) provides the mass conservation equation applied to the solute in the mobile water alone:

$$\theta_m \frac{\partial C}{\partial t} + \frac{\Delta \theta_{im}}{\Delta t} C^{*} = -\underline{v}_D \cdot \underline{\nabla} C + \underline{\nabla} \cdot \left(\theta_m \underline{\underline{D}}_h \cdot \underline{\nabla} C\right) + q(C' - C) - \lambda \theta_m C - \alpha(C - C_{im}) + \left(F \frac{\partial h}{\partial t} - \frac{\partial \theta_m}{\partial t}\right) C \quad (17)$$

It is still necessary to discuss the last term of the right-hand side of Equation (17). In the saturated zone, the water content terms (θ, θ_m, θ_{im}) are assumed constant and $F \approx S_s$. In that case:

$$\left(F \frac{\partial h}{\partial t} - \frac{\partial \theta_m}{\partial t}\right) C \approx S_s \frac{\partial h}{\partial t} C \approx S_s \frac{\Delta h}{\Delta t} C \quad (18)$$

Since S_s is small, this term is often negligible. In that case, Equation (17) reduces to the "classical" solute transport equation in the presence of a dual-porosity process:

$$\theta_m \frac{\partial C}{\partial t} = -\underline{v}_D \cdot \underline{\nabla} C + \underline{\nabla} \cdot \left(\theta_m \underline{\underline{D}}_h \cdot \underline{\nabla} C \right) + q(C' - C) - \lambda \theta_m C - \alpha (C - C_{im}) \quad (19)$$

In the unsaturated zone, one can write:

$$\theta = \theta_m + \theta_{im} + \theta_c \quad (20)$$

where θ_c represents a possible portion of isolated water, which does not contribute at all to transport processes. This quantity of water can be assumed as either negligible or invariant with time, for which case one can write,

$$F \frac{\partial h}{\partial t} \approx \frac{\partial \theta}{\partial t} = \frac{\partial \theta_m}{\partial t} + \frac{\partial \theta_{im}}{\partial t} \approx \frac{\Delta \theta_m}{\Delta t} + \frac{\Delta \theta_{im}}{\Delta t} \quad (21)$$

Introducing Equation (21) into Equation (17) provides the mathematical form of the transport equation in the mobile water, in the unsaturated zone:

$$\theta_m \frac{\partial C}{\partial t} = -\underline{v}_D \cdot \underline{\nabla} C + \underline{\nabla} \cdot \left(\theta_m \underline{\underline{D}}_h \cdot \underline{\nabla} C \right) + q(C' - C) - \lambda \theta_m C - \alpha (C - C_{im}) + \frac{\Delta \theta_{im}}{\Delta t} \left(C - C^* \right) \quad (22)$$

The last term of the right-hand side exists when the transfer of water occurs from the immobile water to the mobile water (i.e. $\Delta \theta_{im} / \Delta t < 0$, $C^* = C_{im}$), the solute present in the mobile water being diluted or concentrated depending whether $C > C_{im}$ or not. If water is transferred from the mobile to the immobile water, the concentration in the mobile water is not affected by loss of a portion of this phase.

Different numerical approaches can be found in the literature for the solution of the dual-porosity, first-order transfer model, differing from a point of view of computational efficiency and stability (Gallo et al. 1996). A first solution is to use a fully coupled approach (Gambolati et al. 1994) for which the concentration in the immobile water C_{im}^* is considered as a state variable just like the concentration in the mobile water C. The number of unknowns changes from N to $2N$ (N being the number of nodes in the discretization), which increases considerably the size of the equation system to be solved and therefore the demand on

memory and computation time. Decoupled approaches give very accurate results at lower computational costs. Gambolati et al. (1993) use an integro-differential approach that allows an analytical computation of concentrations in the immobile water over a time step. The resulting expression is then back-substituted into the equation relative to the concentration evolution in the mobile water. Unfortunately, this numerical scheme shows instabilities if the first order transfer coefficient between mobile and immobile water becomes large. Ibaraki and Sudicky (1995) or Gambolati et al. (1996) propose a decoupled approach for which the differential equation relative to mass-conservation in the immobile water (Equation 14) is approximated by a finite difference scheme written over the computation time step. Once more, the resulting expression is back-substituted into the equation describing the evolution of concentration in the mobile water (Equation 17). This approach gives very accurate results and shows a very good stability.

A fourth approach proposed by Biver (1993) is used in the SUFT3D code. A semi-analytical expression is found for the concentration evolution in the immobile water (Equation 16) over the computation time step. The resulting expression is substituted in Equation 17. The resulting partial differential equation is then solved using the finite element method. Details can be found in Brouyère (2001). The coding of the dual-porosity concept in the SUFT3D code was verified by comparison with the analytical solutions proposed by van Genuchten and Wierenga (1976), using the CXTFIT code (Toride et al. 1995) and by comparison with FRAC3DVS (Therrien 1992, Therrien and Sudicky 1996) based on the computation of a synthetic radially converging tracer experiment (Brouyère et al. 2000).

3 Modelling tracer experiments performed in the chalk

Details about the tracer experiments performed in the unsaturated zone overlying the Hesbaye aquifer in Belgium can be found in Brouyère (2001) and Brouyère et al. (2004a). After a short

description of the experimental setup, the simulations of the experiments performed with the SUFT3D code are described and discussed.

3.1 Tracer experiments performed in the chalk

In the Hesbaye region, the geological succession consists, from top to bottom, of 13 m of loess formations, 2 to 4 m of flint conglomerate and 32 m of fissured chalk. The aquifer, located in the fissured chalk, is unconfined. The aquifer basis is formed by several meters of smectite clay (Brouyère et al. 2004b). The experimental site, located at Bovenistier, is equipped with 7 boreholes drilled and screened at different depths in the saturated zone (the central well PC and two piezometers Pz CS and Pz 12) and in the unsaturated zone (Pz CNS in the unsaturated chalk, Pz CGL in the flint conglomerate, Pz LB and Pz LS in the loess). Undisturbed core samples were collected during the drilling of the boreholes for laboratory measurements, such as hydraulic conductivity measurements, the determination of unsaturated properties of the different geological formations and the analysis of nitrate and pesticide contents. In the field, infiltration tests were performed in the unsaturated zone and pumping tests were performed in the saturated zone. Tracer experiments were performed in both the unsaturated and saturated zone. Table 1 summarizes the information relative to these tracer injections.

Two tracer tests were performed between Pz CS and the central well in the saturated zone of the chalk aquifer, in radially converging flow conditions. For the first injection (phase 1 in Table 1), eosin Y was used and the pumping rate at the recovery well was 1.2 m^3/h. For the second injection (phase 2 in Table 1), naphtionate was used and the pumping rate at the recovery well was 6 m^3/h. Figure 5 presents the measured breakthrough curves at the central well PC.

Two tracer injections were performed in the unsaturated chalk, from Pz CNS (Figure 6). For the first injection with potassium chloride (KCl), artificial recharge conditions were created

by adding water at a constant rate (0.3 m^3/h) in the well after tracer injection. This led to enhanced hydraulic gradient between the injection point and the aquifer and locally to a higher degree of saturation in the unsaturated chalk. As the chalk layer is overlain by a thick loess formation, actual recharge conditions are likely to be less intensive. A second tracer injection was performed using potassium iodide (KI), without addition of water after tracer injection. This configuration reflects better the actual seepage conditions in the unsaturated chalk. The first tracer experiment in the unsaturated chalk was performed during a period of low groundwater levels that prevailed during the whole tracer monitoring period (3 days). For this experiment, the unsaturated thickness of chalk crossed by the tracer was approximately 8.5 m. For the second tracer experiment in the unsaturated chalk, the iodide tracer was also injected at the period of low groundwater levels. However, the duration of the test was longer (about two years) and a progressive rise in groundwater levels was observed in the aquifer during that period. The unsaturated thickness of chalk, so the distance travelled by the tracer, was reduced down to 4 to 3 m.

3.2 Conceptual model and discretisation

Three finite element meshes were used for modelling exercise: a regional mesh and two local meshes, both centred around the central well and refined in the area of the tracer experiments. The regional model was developed using a finite element mesh with an horizontal extension of 320 m × 320 m and a vertical dimension of 32 m representing the saturated zone of the aquifer. This model, used for calculating groundwater heads at the boundaries of the two local meshes, was calibrated for natural groundwater flow conditions, based on water levels measured in the region during the period of the experiments and on pumping tests performed in the central well (results not shown). In order to account for the rock alteration and strain relaxation at shallow depth, values of hydraulic conductivity defined in the upper layers are higher (between 1.0×10^{-4} and 4.0×10^{-4} $m.s^{-1}$) than in the deepest layers (between 5.0×10^{-5} and

1.0×10^{-4} m.s^{-1}). The hydraulic conductivity field obtained from the calibration of the regional model was transferred to the corresponding finite elements of the local meshes.

Tracer tests performed in the saturated zone were modelled using a finite element mesh with an horizontal extension of 80 m × 80 m and a vertical dimension of 32 m representing the saturated zone of the chalk aquifer (10 layers of finite elements ranging from 2 m to 5 m). Tracer tests performed in the unsaturated chalk were modelled using another mesh with a horizontal extension of 18 m × 18 m, extending over the whole thickness of the saturated and unsaturated zone (50 m). In the unsaturated zone, the discretisation is made of 1 m × 1 m × 1 m cubic finite elements.

At the lateral boundaries of the local meshes, prescribed heads (Dirichlet boundary conditions) were defined in the saturated zone. Head values were set equal to those computed, at the same location, using a "regional" model run with the same stress factors (recharge, pumping rate…). In the unsaturated zone, water fluxes being essentially vertical, lateral faces were considered as impervious. At the top of the model, a flux-type (Neumann) boundary condition was prescribed. The transient nature of recharge conditions was not considered and a mean annual rate of 9.5×10^{-9} m/s was applied (approx. 300 mm/year).

The characteristic curves $\theta(h)$ and $k_r(\theta)$ were defined for each geological formation encountered, together with an estimation of the saturated hydraulic conductivity K_S. For the loess formations, van Genuchten relationships were used, considering the mean estimates of the parameters obtained by fitting this relationship on retention curves that were measured on loess samples (Brouyère et al. 2004a). In the absence of data, the flint conglomerate was considered as a silty sand for which mean van Genuchten parameters were taken from tables provided by Carsel and Parrish (1988). For the chalk, a bimodal relationship similar to that established in section 2.1 was considered. Parameter values considered for the different geological formations are summarized in Table 2.

Saturated hydraulic conductivity values for the loess and conglomerate formations were obtained by modelling constant head infiltration tests performed in the field. Calibrated hydraulic conductivity values are in good agreement with those derived from infiltration tests (Brouyère 2001, Brouyère et al. 2004a): 1.5 to 5.0×10^{-7} m/s for the loess formation and 2.0×10^{-6} m/s for the flint conglomerate. For the unsaturated chalk, the infiltration tests provided an estimation of saturated hydraulic conductivity that was considered too low compared to values derived from the pumping tests. It was decided to use a mean hydraulic conductivity $K_S = 1.0\times10^{-4}$ m/s.

3.3 Modelling tracer experiments performed in the saturated chalk

The two tracer experiments performed between Pz CS and the central well were modelled with the SUFT3D code, using the CDPM approach. Figure 5 shows the comparison between measured and fitted breakthrough curves. Table 3 summarizes adjusted hydrodispersive parameters.

The calibrated effective porosity is low, typical for the fissure porosity of the chalk. First arrivals are not perfectly calibrated because the mesh is not refined enough for modelling the low dispersive transport along fissures between Pz CS and the central well. Because of numerical dispersion, reducing further the value of longitudinal dispersivity α_L (L) did not have any effect on the computed breakthrough curve. The calibrated longitudinal dispersivity coefficient is thus probably overestimated. The calibrated first-order transfer coefficient α is in a good agreement with values found for other tracer experiments performed in the fissured chalk in the Hesbaye aquifer (Biver 1993, Hallet 1999). The porosity associated with the immobile water θ_{im} is relatively small. However, in the saturated zone, the dual-porosity concept is usually considered as a diffusive process characterised by relatively slow kinetics. Because the tracers were injected very close to the recovery well, the mean travel time in the

aquifer is very short. It is thus likely that a part of the immobile water does not take part in the retardation process. The calibrated immobile water porosity thus reflects the quantity of water that is involved in the physical retardation process rather than the total quantity of immobile water.

3.4 Modelling tracer experiment performed in the unsaturated chalk under artificial injection conditions

Steady state conditions were assumed for modelling the tracer experiment in the unsaturated chalk for high recharge rates. Tracer injection and water recharge conditions were modelled considering a nodal source term applied at the finite element node which is the nearest from the screen level of Pz CNS in the three-dimensional finite element mesh. A constant rate of 0.3 m^3/h was applied in the model. A tracer injection duration of one hour was considered (close to the actual 53 min. that were actually needed to inject the 300 litres of tracer fluid). The calibration was based on the fitting of the chloride breakthrough curve, this tracer being considered as conservative (i.e. no sorption or degradation). First, the CDPM approach was considered, assuming that effective porosity and immobile water porosity are constant values defined at the R.E.V. scale, independent of the rock saturation. In this case, the degree of saturation plays only a role for the computation of Darcy fluxes. The fitting parameters are the effective porosity, the longitudinal dispersivity, the immobile water porosity and the first order transfer coefficient between mobile and immobile water phases. Second, the DDPM approach, as described in the previous sections, was considered. In this case, the saturation degree of the rock plays a role on both the computation of Darcy fluxes (groundwater flow computation) and on the distribution of water between mobile and immobile porosity (transport computation). The magnitudes of effective porosity and immobile water porosity are not exactly known. The only information is the partitioning coefficient c_{part} considered as a fitting parameter together with the longitudinal dispersivity and the first-order transfer

coefficient. Figure 6a presents the chloride breakthrough curve measured in the field together with the best fit obtained (by trial-and-error) considering the two approaches. Table 3 summarizes the calibrated parameters.

For the CDPM approach, fitted parameters are close to those obtained from modelling the tracer experiments performed in the saturated zone (see Table 3). The effective porosity is low (fissure porosity) and the longitudinal dispersivity coefficient is relatively small but probably overestimated again. The immobile water porosity is similar to that considered in the saturated zone, reflecting some bypass of the immobile water during the tracer downward migration in the unsaturated chalk. The first order transfer coefficient is very similar to that obtained in the saturated zone. This indicates that hydrodispersive processes governing the mobility of tracers during these experiments were similar to those prevailing in the saturated zone: a fast, preferential migration of tracers along partially or fully saturated fissures and a strong physical retardation in the immobile water located in the matrix porosity.

When the DDPM approach is considered, a partitioning coefficient c_{part} = 0.02 is found. This indicates that the effective porosity is small and the immobile water porosity is large (see Figure 4). At the same time, the calibrated first order transfer coefficient is smaller than that obtained from the CDPM approach. In fact, the degree of saturation varies spatially and therefore also the distribution of porosity between mobile and immobile water and the hydraulic conductivity. For lower degrees of saturation, the effective porosity is larger. This contributes to the retardation of that portion of the tracer migrating across these zones, as compared to the quantity of tracer migrating across zones characterised by a higher degree of saturation. The DDPM approach thus requires less ‘diffusive’ effect for modelling tracer late arrivals compared to the CDPM approach. At the extreme, delayed tracer arrivals could be obtained just by adapting the hydraulic conductivity functionality and the partitioning coefficient until the breakthrough curve is reproduced independently from any dual-porosity

effect. However, it is not realistic to think that diffusion into the immobile water does not have any influence on the mobility and retardation of tracers in the chalk.

Whatever the modelling approach that is considered (CDPM or DDPM), modelling results confirm the conceptual model of tracer transport for intensive recharge conditions. The fissure network was active, driving tracers at high velocities across the unsaturated zone, together with an important dual-porosity effect that produced physical retardation due to storage of tracers in the immobile water located in the low permeability matrix. It has to be mentioned that previous attempts, consisting of modelling the unsaturated properties of the chalk with 'classical' functionalities (such as unimodal van Genuchten relationships) were unable to explain and reproduce short travel times such as those observed in the field (Crispin 2000). The bimodal functionality developed to model the behaviour of the variably saturated chalk is thus one of the key factors that allow modelling of the tracer experiments. It allows a fair reproduction of the very dynamic behaviour of the variably saturated chalk when the saturation degree varies. A full dual-permeability approach, modelling the chalk by two flow continua (one for the matrix, one for the fissured component) like that of Gerke and van Genuchten (1993) could probably also provide an even better representation of the phenomena but the required data are generally not available.

3.5 Modelling of the tracer experiment performed in the unsaturated chalk for natural infiltration conditions

This tracer experiment is more representative of natural downward migration conditions of solute contaminants in the unsaturated chalk. Because the tracer experiment lasted for two years, the interpretation and modelling should ideally consider the transient nature of recharge conditions and the variations in piezometric levels. However, for computation time and numerical reasons, simplified assumptions were considered. First, as no detailed data were available on the evolution of water contents with time in the unsaturated zone, the transient

nature of the recharge was neglected. Second, as mentioned previously, in order to save memory and computation time, a local model was needed for the transport simulations. At the limits of this local model, boundary conditions were not easy to define in the fluctuating zone of the groundwater table. Normally, boundary conditions should be switched from impervious to prescribed head as the groundwater table rises, but this was not available in the SUFT3D. In a first attempt, the rise of the groundwater table was considered by increasing the total head prescribed at the Dirichlet nodes. With such a configuration, water could enter or leave the model via the bottom layers only, resulting in very artificial Darcy fluxes and pressure fields, with the direct consequence that numerical problems were inevitable in the transport simulations.

Steady state groundwater flow simulations were finally performed, considering groundwater levels prevailing at the beginning of the tracer experiments (low groundwater levels). For the transport simulations, the size of the time steps was restricted to 1 hour because of the numerical Courant criterion. With the total simulation time being 2 years, very long computation times of approximately one week were required.

Because of the above restrictions, the objectives of the transport simulations performed in natural infiltration conditions were to check: (1) if the strong contrast observed in terms of travel times across the unsaturated chalk could be reproduced; (2) to check the consistency of the conceptual model postulating that contaminants migrate across the matrix in natural recharge conditions; and (3) to have an estimation of the effective porosity associated to the chalk in natural infiltration conditions. For the simulations, unless stated here after, hydrodispersive parameters were set equal to those obtained when modelling the tracer experiments performed under intense injection conditions.

Using the DDPM approach with the hydrodispersive parameters obtained for the tracer experiments performed under experimental intense injection conditions did not result in any significant tracer arrival during the sampling campaign (almost 2 years).

Different simulations were performed considering the CDPM approach. It was first considered that all the water located in the chalk was mobile (no dual-porosity effect). Practically, a value of 35% was defined for the effective porosity. As for the DDPM approach, the result of this simulation did not show any significant tracer arrival at the pumping well during the period corresponding to the sampling campaign. The second test performed with the CDPM approach consisted in trying to obtain a modelled first arrival of the order of the observed one, by adjusting the effective and the immobile water porosity. This was obtained by using an effective porosity of 10% and an immobile water porosity of 15% in the model (Figure 6b). The order of magnitude of the first arrival is respected (almost one year). However, the modelled breakthrough curve shows an evolution that departs from the measured one, the latter being sharper. This is probably related to the fact that tracer arrivals were not only explained by the downward migration of the tracer in the unsaturated zone, but also by the rise of the groundwater table that washed the tracer during its downward migration in the unsaturated zone.

The effective porosity (10%) obtained by adjusting the first arrival is too small to be representative of the matrix porosity. However, as stated before, groundwater levels prevailing at the beginning of the tracer experiment were considered in the simulations. Because of that, the travel distance in the model (approximately 9m) is almost 3 times the actual distance covered by the tracer (approximately 3m). A simple rule of three thus provides a rough estimation of 30% for the effective porosity from the 10% obtained with the model, which is in better agreement with the estimated chalk matrix porosity.

From the analysis of these simulations, it can be concluded that, for natural infiltration conditions, solute contaminant downward migration occurs across the chalk matrix, as suggested in the conceptual model proposed by Brouyère et al. (2004a).

4 General conclusions

This research has provided several very useful contributions. First, a new functionality is proposed for modelling the fundamental unsaturated properties (retention curve and hydraulic conductivity curve) for structured formations such as fissured rocks or macroporous soils. This functionality allows an analytical evaluation of the hydraulic conductivity curve from the retention curve and it is continuously derivable over the whole range of water contents. It reproduces naturally the fast and strong variation in hydraulic conductivity that is often observed in structured media when the preferential flow paths become desaturated. Second, a generalisation of the dual-porosity model is proposed to the case of variably saturated groundwater flows, in a way that is similar to that proposed by Zurmülh and Durner (1996). Third, the mathematical formulation and the numerical implementation of all these developments in the three-dimensional groundwater flow and transport simulator SUFT3D are described. All these developments are used to provide an innovative and unified point of view on the hydrodynamic and hydrodispersive behaviour of variably saturated dual-porosity, dual-permeability chalk.

The modelling results obtained for the different tracer experiments performed in the saturated and the unsaturated chalk at Bovenistier under various experimental conditions confirm that the conceptual model proposed by Brouyère et al. (2004a) is valid to explain the hydrodispersive behaviour of the chalk for variably saturated conditions. In the saturated zone and in the unsaturated zone when intensive recharge conditions prevail, the order of magnitude of the hydrodispersive parameters shows that the fissure network drives the mobility of contaminants. At the same time, the matrix acts as a buffer where these

contaminants are temporarily stored and retarded. Under natural infiltration conditions, the fissure network is inactive and tracers migrate slowly downward across the high porosity, low permeability chalk matrix.

The analysis and interpretation of the tracer experiments performed in the chalk could be improved by considering several factors that were neglected, such as tracer density effects, the transient nature of the groundwater recharge and variations in groundwater levels. It could be interesting to perform further numerical simulations using the DDPM approach for explaining the tracer experiments performed in natural recharge conditions. A comparison between the present approach and multi-continuum approaches could provide a better understanding of the possible influence of pressure disequilibrium between the fissures and the matrix (bypass flow) on the mobility and retardation of contaminants.

In the field, a better understanding and quantification of the behaviour of the chalk under variably saturated flow could be obtained by performing tracer injections under variable recharge conditions. In order to monitor the impact of the fissure network inactivation, it could be interesting to perform tracer injections with variable artificial recharge rates or to perform a long duration tracer injection during which the artificial recharge is stopped at a time when tracer arrivals are still clearly above the detection limit. This kind of experiment would be similar to flow interruption methods such as proposed by Brusseau et al. (1989) or Cote et al. (2000), used to quantify kinetic retardation processes affecting the behaviour of solutes in column experiments. Such experiments could contribute to a better assessment of the functionality used for porosity partitioning and to a better understanding of fissure-matrix interactions.

The model presented here could be used to study the impact of groundwater table seasonal variations on the evolution of contaminant concentrations such as nitrates. This could be of direct interest for the estimation of groundwater quality trends (seasonal detrending). The

model is also compatible with the research works of Tokunaga and Wan (1997), Tokunaga et al. (2000), Price et al. (2000) or Tokunaga and Wan (2001). The developments presented here could thus be adapted to provide the mathematical framework for these researches.

Acknowledgement

The researches of S. Brouyère were supported by a 4 year PhD grant provided by the National Funds for Scientific Research of Belgium. Recent developments of this research were also financed by the European FP6 Project 505428 (GOCE) AQUATERRA. The author would like to thank Vincent Hallet, Ivette Bauthière, Martin Sauter and an anonymous reviewer for their fruitful comments and corrections on the initial version of the manuscript.

References

Bai, M., Elsworth, D., Roegiers, J.-C., Multiporosity/multipermeability approach to the simulation of naturally fractured reservoirs, Water Resour. Res., 29(6), 1621-1633, 1993.

Berkowitz, B., Bear, J., Braester, C., Continuum models for contaminant transport in fractured porous formations, Water Resour. Res., 24(8), 1225-1236, 1988.

Berkowitz, B., Characterizing flow and transport in fractured geological media: A review, Adv. Water Resour., 25, 861-884, 2002.

Biver, P., Etude phénoménologique et numérique de la propagation de polluants miscibles dans un milieu à porosité multiple (phenomenological and numerical study of miscible pollutant transport in a multi-porosity medium), in French, PhD thesis, University of Liège, Faculty of Applied Sciences, 389p, 1993.

Brouyère, S., Dassargues, A., Therrien, R., Sudicky, E.A., Modelling of dual porosity media : comparison of different techniques and evaluation on the impact on plume transport simulations, IAHS Publication nb 265, Ed. F.Stauffer, W.Kinzelbach, K.Kovar & E.Hoehn. IAHS Press, Wallingford, Oxfordshire, UK, 22-27, 2000.

Brouyère, S., Etude et modélisation du transport et du piégeage des solutés en milieu souterrain variablement saturé (study and modelling of transport and retardation of solutes in variably saturated media), in French, PhD Thesis, University of Liège, Faculty of Applied Sciences, 572p, 2001.

Brouyère, S., Modeling tracer injection and well-aquifer interactions: a new mathematical and numerical approach, Water Resour. Res., 39(3), doi:10.1029/2002WR001813, 2003.

Brouyère, S., Dassargues, A., Hallet, V., Migration of contaminants through the unsaturated zone overlying the Hesbaye chalky aquifer in Belgium : a field investigation, J. Contam. Hydrol., vol. 72 (1-4), 135-164, doi: 10.1016/j.conhyd.2003.10.009, 2004a.

Brouyère, S., Carabin, G., Dassargues, A., Climate change impacts on groundwater resources: modelled deficits in a chalky aquifer, Geer basin, Belgium, Hydrogeol. J., 12, 123-134, doi: 10.1007/s10040-003-0293-1, 2004b.

Brusseau, M. L., Rao, P. S. C., Jessup, R. E., Davidson, J. M., Flow interruption: a methods for investigating sorption nonequilibrium, J. Contam. Hydrol., 4, 223-240, 1989.

Carsel, R. F., Parrish, R. S., Developing joint probability distributions of soil water retention characteristics, Water Resour. Res., 24(5), 755-769, 1988.

Celia, M. A., Bouloutas, E. T., Zarba, R. L., A general mass-conservative numerical solution for the unsaturated flow equation, Water Resour. Res., 26(7), 1483-1496, 1990.

Coats, K. H., Smith, B. D., Dead-end pore volume and dispersion in porous media, Soc. Pet. Eng. J., 4, 73-84, 1964.

Cooley, R. L., Some procedures for numerical solution of variably saturated flow problems, , Water Resour. Res., 19(5), 1271-1285, 1983.

Cote, C. M., Bristow, K. L., Ross, P. J., Increasing the efficiency of solute leaching : impacts of flow interruption with drainage of the “preferential flow paths”, J. Contam. Hydrol., 43, 191-209, 2000.

Crispin, C., Modélisation des essais de traçage en Hesbaye : transport des polluants en zone saturée et non saturée (Modelling tracer experiments in the Hesbaye aquifer : pollutant transport in the saturated and unsaturated zones), in French, Master thesis (D.E.S.), University of Liège, Faculty of Applied Sciences, 84p, 1999.

Diersch, H.-J.G., Perrochet, P., On the primary variable switching technique for simulating unsaturated-saturated flows, Adv. Water Resour., 23, 271-301, 1999.

Diersch, H.J.G., About the difference between the convective form and the divergence form of the transport equation. In: FEFLOW White Papers, Vol. I, Berlin: WASY Ltd, 119-130 [Chapter 6], 2001.

Durner, W., Hydraulic conductivity estimation for soils with heterogeneous pore structure, Water Resour. Res., 30(2), 211-223, 1994.

Dykhuizen, R. C., Transport of solutes through unsaturated fractured media, Water Res., 21(12), 1531-1539, 1987.

Dykhuizen, R. C., A new coupling term for dual-porosity models, Water Resour. Res., 26(2), 351-356, 1990.

Finsterle, S., Using continuum approach to model unsaturated flow in fractured rock, Water Resour. Res., 36(8), 2055-2066, 2000.

Fredlung, D. G., Xing, A., Equations for the soil-water characteristic curve, Can. Geotech. J., 31, 521-532, 1994.

Fredlung, D. G., Xing, A., Huang, S., Predicting the permeability function from unsaturated soils using the soil-water characteristic curve, Can. Geotech. J., 31, 533-546, 1994.

Gallo, C., Paniconi, C., Gambolati, G., Comparison of solution approaches for the two-domain model of nonequilibrium transport in porous media, Adv. Water Resour., 19(4), 241-253, 1996.

Gambolati, G., Putti, M., Paniconi, C., Mass transfer analysis in sorbing porous media by an integro-differential approach, Advances in Hydro-Science and –Engineering, 1, 1819-1828, 1993.

Gambolati, G., Gallo, C., Paniconi, C., Numerical integration methods for the dual porosity model in sorbing porous media, Comput. Methods in Water Resour., X, ed. A. Peters et al., Kluwer Academic Press, Dordrecht, NL, 621-628, 1994.

Gambolati, G., Putti, M., Paniconi, C., Projection methods for the finite element solution of the dual-porosity model in variably saturated porous media, in: Advances in Groundwater Pollution Control and Remediation, NATO-ASI Series 2: Environment, vol.9, ed. M. M. Aral, Kluwer Academic, Dordrecht, Holland, 97-125, 1996.

Gerke, H. H., van Genuchten, M. TH., A dual-porosity model for simulating the preferential movement of water and solutes in structured porous media, Water Resour. Res., 29(2), 305-319, 1993.

Gwo, J.-P., Multi-region flow and transport in subsurface media, Ph.D. thesis, Dpt of Civil and Environmental Engineering, Pennsylvania State University, 283p, 1992.

Hallet, V., Etude de la contamination de la nappe aquifère de Hesbaye par les nitrates: hydrogéologie, hydrochimie et modélisation mathématique des écoulements et du transport en milieu saturé (Contamination of the Hesbaye aquifer by nitrates: hydrogeology, hydrochemistry and mathematical modeling), in French, PhD Thesis, University of Liège, Faculty of Sciences, 361p, 1999.

Huyakorn, P. S., Mercer, J. W., Ward, D. S., Finite element matrix and mass balance computational schemes for transport in variably saturated porous media, Water Resour. Res., 21(3), 346-358, 1985.

Ibaraki, M., Sudicky, E. A., Colloid-facilitated contaminant transport in discretely fractured porous media. I: Numerical formulation and sensitivity analysis, Water Resour. Res., 31(12), 2945-2960, 1995.

Letniowski, F. W., Forsyth, P. A., A control volume finite element method for three-dimensional NAPL groundwater contamination, Int. J. Num. Met. Fl., 13, 955-970, 1991.

Mallants, D., Tseng, P.-H., Toride, N., Timmerman, A., Feyen, J., Evaluation of multimodal hydraulic functions in characterizing a heterogeneous field soil, J. Hydrol., 195, 172-199, 1997.

Mualem, Y., A new model for predicting the hydraulic conductivity of unsaturated porous media, Water Resour. Res., 12(3), 513-522, 1976.

Or, D., Tuller, M., Flow in unsaturated fractured porous media: hydraulic conductivity of rough surfaces, Water Resour. Res., 36(5), 1165-1177, 2000.

Othmer, H., Diekkrüger, B., Kutilek, M., Bimodal porosity unsaturated hydraulic conductivity, Soil Sci., 152(3), 139-150, 1991.

Paniconi, C., Aldama, A. A., Wood, E. F., Numerical evaluation of iterative and noniterative methods for the solution of the nonlinear Richards equation, Water Resour. Res., 27(6), 1147-1163, 1991.

Paniconi, C., Putti, M., A comparison of Picard and Newton iteration in the numerical solution of multidimensional variably saturated flow problems, Water Resour. Res., 30(12), 3357-3374, 1994.

Peters, R. R., Klavetter, E. A., A continuum model for water movement in an unsaturated fractured rock mass, Water Resour. Res., 24(3), 416-430, 1988.

Price, M., Downing, R. A., Edmunds, W. M., The chalk as an aquifer, in: The hydrogeology of the chalk of north-west Europe, Ed. Downing, Price, Jones, Oxford Science Publ., Clarendon Press, Oxford, U.-K., 35-58, 1993.

Price, M., Low, R. G., McCann, C., Mechanisms of water storage and flow in the unsaturated zone of the Chalk aquifer, J. Hydrol., 233, 54-71, 2000.

Pruess, K., Faybishenko, B., Bodvarsson, G.S., Alternative concepts and approaches for modelling flow and transport in thick unsaturated zones of fractured rocks, J. Contam. Hydrol., 38, 281-322, 1999.

Putti, M., Paniconi, C., Evaluation of Picard and Newton iteration schemes for three-dimensional unsaturated flow, in Procceedings of the IX International Conference on Computational Methods in Water Resources, vol. 1, Numerical Methods in Water Resources, edited by G. Gambolati, A. Rinaldo, C. A. Brebbia, W. G. Gray, and G. F. Pinder, pp. 529-536, Computational Mechanics Publications, Billerica, Mass., 1992.

Rao, P. S. C., Green,, R. E., Ahuja, L. R., Davidson, J. M., Evaluation of a capillary bundle model for describing solute dispersion in aggregated soils, Soil Sci. Soc. Am. J., 40, 815-820, 1976.

Ross, P. J., Smettem, R. J., Describing soil hydraulic properties with sums of simple functions, Soil Sci. Soc. Am. J., 57, 26-29, 1993.

Saaltink, M. W., Carrera, J., Olivella S., Mass balance errors when solving the convective form of the transport equation in transient flow problems, Water Resour. Res., 40, W05107, doi:10.1029/2003WR002866, 2004.

Smettem, K. R. J., Kirkby, C., Measuring the hydraulic properties of a stable aggregated soil, J. Hydrol., 117, 1-13, 1990.

Therrien, R., Three-dimensional analysis of variably-saturated flow and solute transport in discretely-fractured porous media, Ph.D. thesis, University of Waterloo, Dpt of Earth Sciences, 1992.

Therrien, R., Sudicky, E. A., Three-dimensional analysis of variably-saturated flow and solute transport in discretely-fractured porous media, J. Contam. Hydrol., 23, 1-44, 1996.

Tokunaga, T. K., Wan, J., Water film flow along fracture surfaces of porous rock, Water Resour. Res., 33(6), 1287-1295, 1997.

Tokunaga, T. K., Wan, J., Mechanisms for fast flow in unsaturated fractured rock, in: 5th International Symposium on reservoir wettabillity and its effect on oil recovery (Trondheim, Norway, 22-24 juin 1998), 109-117, 1998.

Tokunaga, K. T., Wan, J., Sutton, S. R., Transient film flow on rough fracture surfaces, Water Resour. Res., 36(7), 1737-1746, 2000.

Tokunaga, K. T., Wan, J., Surface-zone flow along unsaturated rock fractures, Water Resour. Res., 37(2), 287-296, 2001.

Toride N., Leij F. J., van Genuchten M. Th., The CXTFIT Code for Estimating Transport Parameters from Laboratory or Field Tracer Experiments, Version 2.0, Research Report No. 137, U.S. Salinity Laboratory, USDA, ARS, Riverside, CA, 121p, 1995.

Vanderkwaak, J. E., Forsyth, P. A., MacQuarrie, K. T. B., Sudicky, E. A., WatSolv sparse matrix iterative solver, User's guide for version 2.16, University of Waterloo, Waterloo, Ontario, Canada, 22p, 1997.

Vanderkwaak, J. E., Numerical simulation of flow and chemical transport in integrated surface-subsurface hydrologic systems, PhD Thesis, University of Waterloo, Department of Earth Sciences, 217p, 1999.

Van Genuchten, M. Th., A closed-form equation for predicting the hydraulic conductivity of unsaturated soils, Soil Sci. Soc. Am. J., 44, 892-898, 1980.

Van Genuchten, M. Th., Wierenga, P. J., Mass transfer studies in sorbing porous media : I. Analytical solutions, Soil Sci. Soc. Am. J., 40, 473-480, 1976.

Wang, J. S. Y., Narasimhan, T. N., Hydrologic mechanisms governing fluid flow in a partially saturated, fractured, porous medium, Water Resour. Res., 21(12), 1861-1874, 1985.

Yeh, G.-T., A lagrangian-eulerian method with zoomable hidden fine mesh approach to solving advection-dispersion equations, Water Resour. Res., 26(6), 1133-1144, 1990.

Younger, P. L., Elliot, T., Chalk fracture system characteristics : implications for flow and solute transport, Q. J. Eng. Geol., 28, S39-S50, 1995.

Zurmühl, T., Durner, W., Modeling transient water and solute transport in biporous soil, Water Resour. Res., 32(4), 819-829, 1996.

Annex 1: Mathematical expressions used to compute the derivatives of the retention curve and the hydraulic conductivity curve

As mentioned previously, the numerical solution of Richards' equation using Newton-Raphson linearization technique needs computation of the derivatives of the retention curve and the hydraulic conductivity curve according to the water content. For completeness, the expressions are provided here after.

When fissures are fully desaturated and the matrix is partially saturated with water:

$$\frac{d\theta}{dh} = \frac{-\alpha_M m_M \left(\theta_{s,M} - \theta_r\right)}{1 - m_M} \Theta_M^{1/m_M} \left(1 - \Theta_M^{1/m_M}\right)^{m_M} \qquad \text{(A.1)}$$

$$\frac{dk_r}{dh} = \frac{dk_r}{d\theta}\frac{d\theta}{dh} = \left(\frac{P}{\theta_s - \theta_r} S_e^{(P-1)} + 2S_e^P \frac{f_I(\theta)}{f(\theta_s)} \frac{d\, f_I(\theta)}{d\theta} \right) \frac{d\theta}{dh} \qquad \text{(A.2)}$$

with :

$$\Theta_M = \frac{\theta - \theta_r}{\theta_{s,M} - \theta_r}$$

$$m_M = 1 - \frac{1}{n_M}$$

$$\frac{d\, f_I}{d\theta} = \alpha_M \left(1 - \Theta_M^{1/m_M}\right)^{(m_M - 1)} \Theta_M^{(1/m_M - 1)}$$

When the matrix is fully saturated and fissures are partially saturated with water :

$$\frac{d\theta}{dh} = \frac{-\alpha_F m_F \left(\theta_s - \theta_{r,F}\right)}{1 - m_F} \Theta_F^{1/m_F} \left(1 - \Theta_F^{1/m_F}\right)^{m_F} \qquad \text{(A.3)}$$

$$\frac{dk_r}{dh} = \frac{dk_r}{d\theta}\frac{d\theta}{dh} = \left(\frac{P}{\theta_s - \theta_r} S_e^{(P-1)} + 2S_e^P \frac{\left(f_I(\theta_J) + f_{II}(\theta)\right)}{f(\theta_s)} \frac{d f_{II}(\theta)}{d\theta} \right) \frac{d\theta}{dh} \qquad \text{(A.4)}$$

with :

$$\Theta_F = \frac{\theta - \theta_{r,F}}{\theta_s - \theta_{r,F}}$$

$$m_F = 1 - \frac{1}{n_F}$$

$$\frac{d f_{II}}{d\theta} = \alpha_F \left(1 - \Theta_F^{1/m_F}\right)^{(m_F - 1)} \Theta_F^{(1/m_F - 1)}$$

Table captions

Table 1. Description of tracer injection performed in the saturated (Pz CS) and in the unsaturated chalk (Pz CNS).

Table 2. Parameters defined for modelling the behaviour of unsaturated formations. For the loess and the flint conglomerate, the van Genuchten – Mualem model is used. For the chalk, the new functionality developed in section 1 is used.

Table 3. Fitted transport parameters for the chalk using the tracer test results. α_L is the longitudinal dispersivity coefficient (L) appearing in the expression of the hydrodynamic dispersion tensor. ([1] Values of effective and immobile water porosity depend of the saturation degree of the rock. This may change from point to point and it is thus impossible to give values for these parameters).

Figure captions

Figure 1. Conceptual model for water recharge and solute transport mechanisms in the variably saturated chalk. Under intensive or artificial recharge conditions, water and contaminants migrate through the saturated fissures and the matrix acts as a buffer zone. Under “natural” recharge conditions, the fissure network is inactive; the migration of water and contaminants is restricted in the matrix.

Figure 2. Illustration of the method used to construct the global retention curve relative to the fissured, dual porosity chalk (dashed line) from the superposition of two van Genuchten retention curves, one for the matrix (light grey curve), one for the fissure (dark grey curve) components. A continuously derivable condition is prescribed at the point (θ_J,h_J).

Figure 3. Unsaturated characteristic curves obtained with $\theta_{s,M}$ = 0.41, α_M =0.099 m^{-1}, n_M =1.1, θ_s =0.42, α_F = 10 m^{-1}. The characteristic curve relative to the matrix and fissure components join at a suction value h_j = 0.4 m, the continuity parameters obtained by solving equations (4a and b) being n_F =3.11 and $\theta_{r,F}$ =0.4088.

Figure 4. Partitioning of water between the mobile and the immobile porosity as a function of the ratio between associated relative hydraulic conductivity values. At saturation (a), the mobile water is associated with the fracture porosity and the dual porosity effect is important; as the rock desaturates (b), the mobile water becomes associated with water in the matrix and the dual porosity effect is reduced.

1 Figure 5. Breakthrough curves of tracers injected in Pz CS during the field tracer experiments
2 (line + symbols) and modelled with the SUFT3D code (dashed lines).
3
4 Figure 6. Breakthrough curves of the tracers injected in Pz CNS under (a) intense artificial
5 recharge conditions and (b) natural recharge conditions (lines + symbols) and modelling
6 results obtained with the SUFT3D code (lines).

Injection well	Pz CS phase 1	Pz CS phase 2	Pz CNS phase 1	Pz CNS phase 2
Injection conditions	Saturated zone	Saturated zone	Artificially intense recharge conditions	Natural recharge conditions
Pumping rate at PC (m^3/h)	1.2	6.0	6.48	Permanent pumping at a rate varying between 3 and 6 m^3/h
Tracer	eosin Y	naphtionate	KCl	I^-
Injected mass (kg)	0.0053	0.0051	100	7.64 (10 of KI)
Tracer volume (m^3)	0.010	0.010	0.3	0.03
Tracer injection duration (h)	0.031 (1min53s)	0.036 (2min11s)	0.88 (53 min)	0.1 (6 min)
Water flush volume (m^3)	0.127	0.132	Constant recharge: 0.1 m^3/h	No recharge
Water flush duration (h)	0.29 (17min20s)	0.22 (12min56s)		
Minimum transit time (h)	0.58 (35min)	0.25 (15min)	5.25	8184 (341 days)
Modal transit time (h)	1.42 (85min)	0.5 (30min)	11,5	15312 (638 days)?

Material		θ_r (-)	$\theta_{s,M}$	$\theta_{r,F}$	θ_s (-)	α_{VG} (m^{-1})	n_{VG} (-)
Loess		0.01	-	-	0.445	3.0	1.14
Flint Conglomerate		0.065	-	-	0.41	1.0	1.89
Fissured chalk	Matrix	0.01	0.40	-	-	0.05	1.1
	Fissures	-	-	0.4088(*)	0.42	10	4.56 (*)
(*) parameters ajusted for garantying continuity at the matching point defined on the matrix and fissure retention curves, for h_J = 0.4 m							

Injection well	Experimental conditions	Modelling approach	θ_m (-)	θ_{im} (-)	α_L (m)	α (s^{-1})
Pz CS	Saturated zone	CDPM	0.004	0.05	1.0	2.0×10^{-7}
PsCNS	Intense recharge	CDPM	0.01	0.08	1.0	2.3×10^{-7}
		DDPM	c_{part} = 0.02[1]		1.0	9.0×10^{-8}
	Natural infiltration	CDPM	0.10	0.15	1.0	2.3×10^{-7}
		DDPM	no tracer arrival observed during the simulated period			

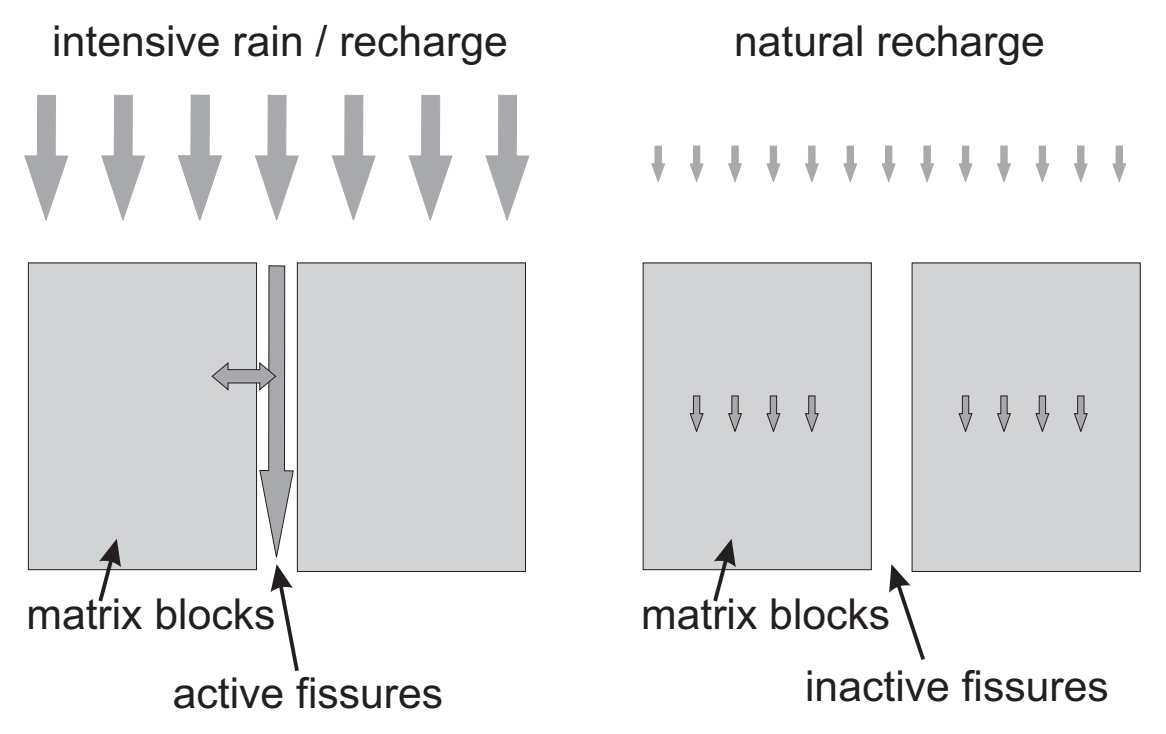
intensive rain / recharge
natural recharge
matrix blocks
active fissures
matrix blocks
inactive fissures

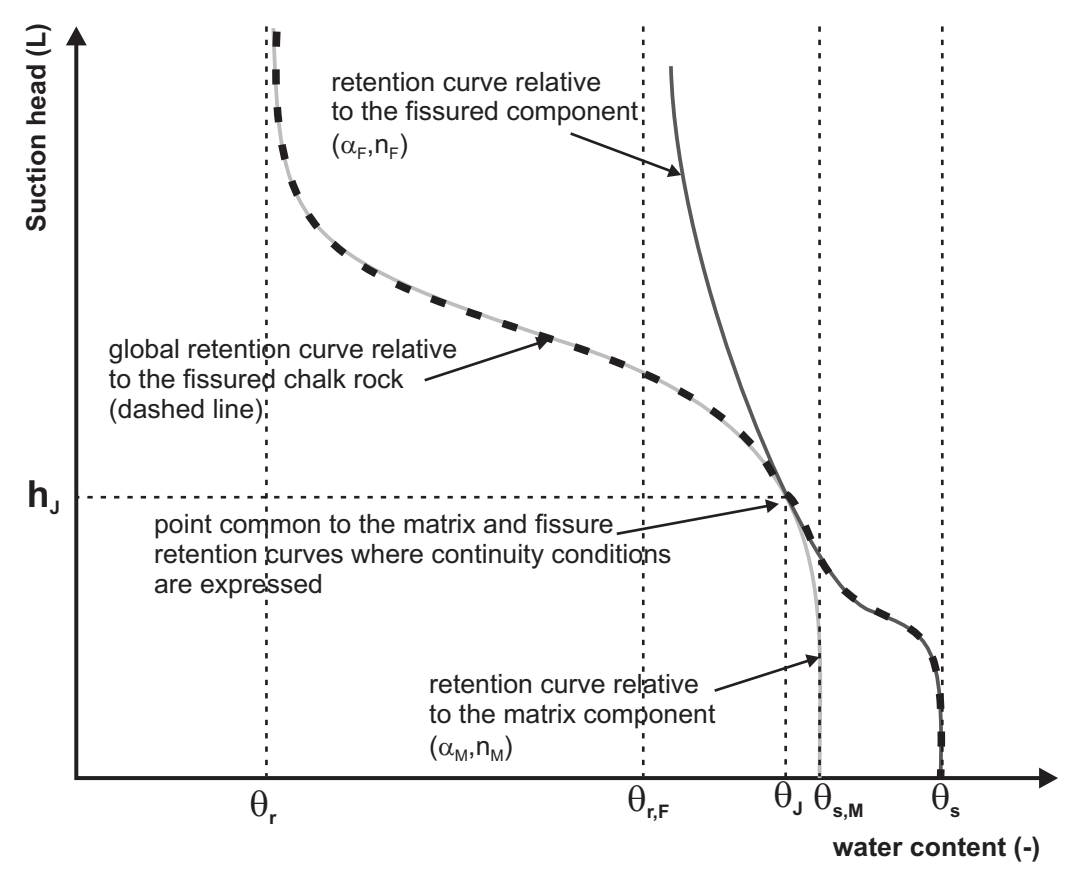
Suction head (L)
retention curve relative to the fissured component (α_F,n_F)
global retention curve relative to the fissured chalk rock (dashed line)
h_J
point common to the matrix and fissure retention curves where continuity conditions are expressed
retention curve relative to the matrix component (α_M,n_M)
θ_r
$\theta_{r,F}$
θ_J
$\theta_{s,M}$
θ_s
water content (-)

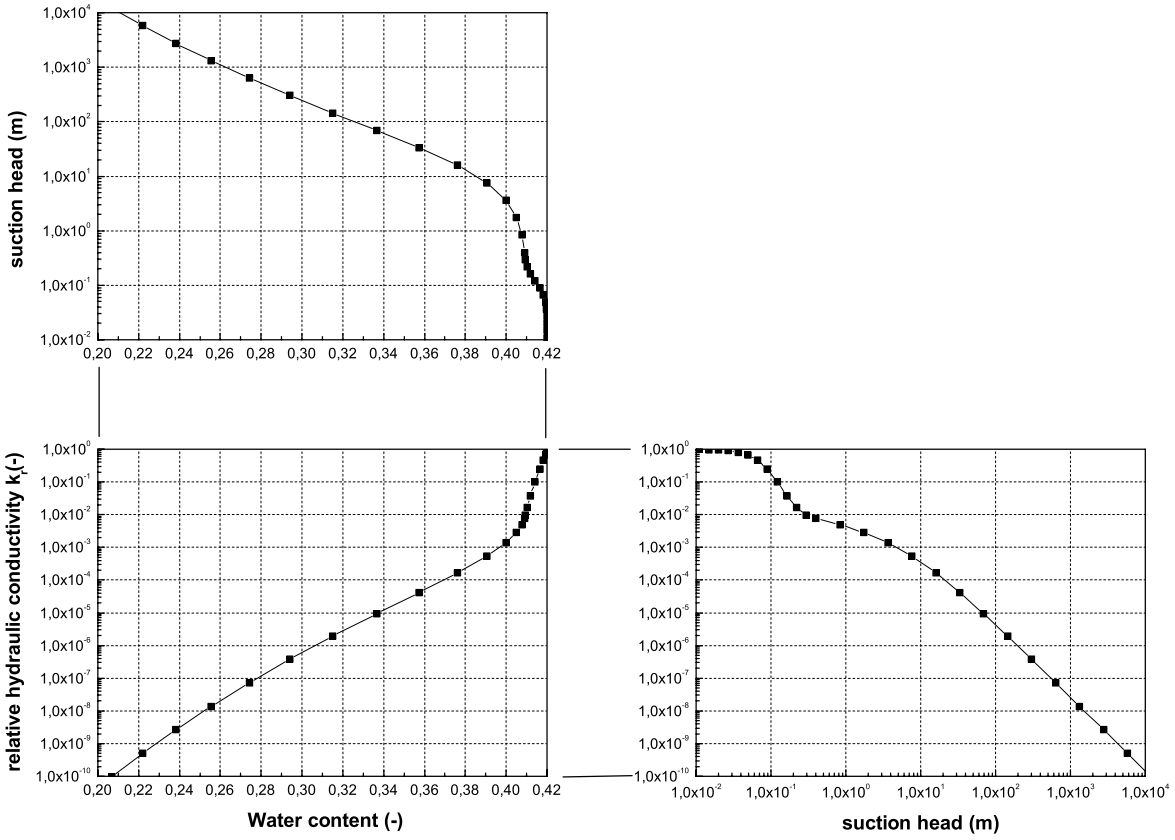
suction head (m)
1,0x10^4
1,0x10^3
1,0x10^2
1,0x10^1
1,0x10^0
1,0x10^-1
1,0x10^-2
0,20 0,22 0,24 0,26 0,28 0,30 0,32 0,34 0,36 0,38 0,40 0,42
relative hydraulic conductivity k_r(-)
1,0x10^0
1,0x10^-1
1,0x10^-2
1,0x10^-3
1,0x10^-4
1,0x10^-5
1,0x10^-6
1,0x10^-7
1,0x10^-8
1,0x10^-9
1,0x10^-10
0,20 0,22 0,24 0,26 0,28 0,30 0,32 0,34 0,36 0,38 0,40 0,42
Water content (-)
1,0x10^-2 1,0x10^-1 1,0x10^0 1,0x10^1 1,0x10^2 1,0x10^3 1,0x10^4
suction head (m)

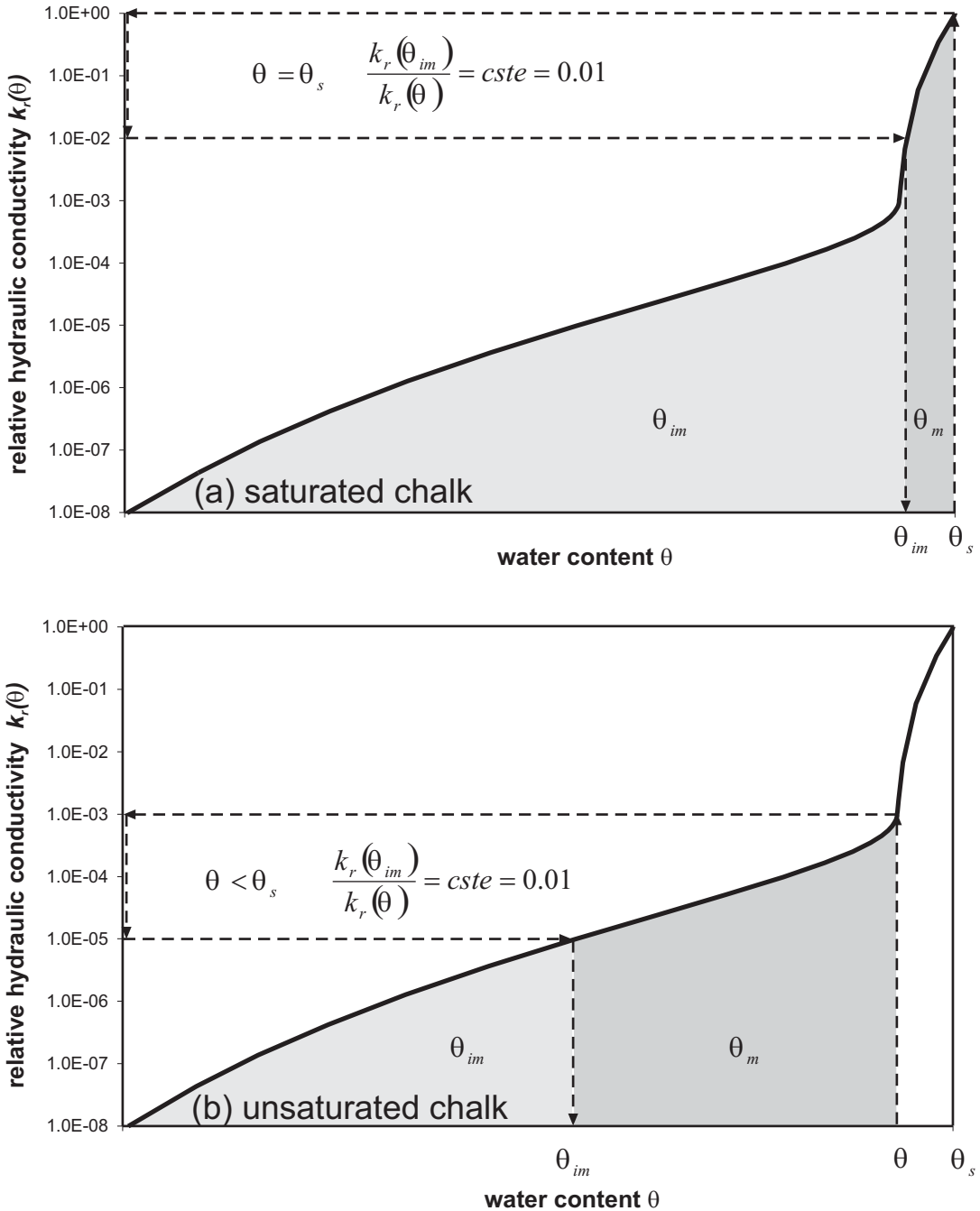
1.0E+00
1.0E-01
1.0E-02
1.0E-03
1.0E-04
1.0E-05
1.0E-06
1.0E-07
1.0E-08
relative hydraulic conductivity $k_r(\theta)$
$\theta = \theta_s$
$\frac{k_r(\theta_{im})}{k_r(\theta)} = cste = 0.01$
θ_{im}
θ_m
(a) saturated chalk
θ_{im}
θ_s
water content θ
1.0E+00
1.0E-01
1.0E-02
1.0E-03
1.0E-04
1.0E-05
1.0E-06
1.0E-07
1.0E-08
relative hydraulic conductivity $k_r(\theta)$
$\theta < \theta_s$
$\frac{k_r(\theta_{im})}{k_r(\theta)} = cste = 0.01$
θ_{im}
θ_m
(b) unsaturated chalk
θ_{im}
θ
θ_s
water content θ

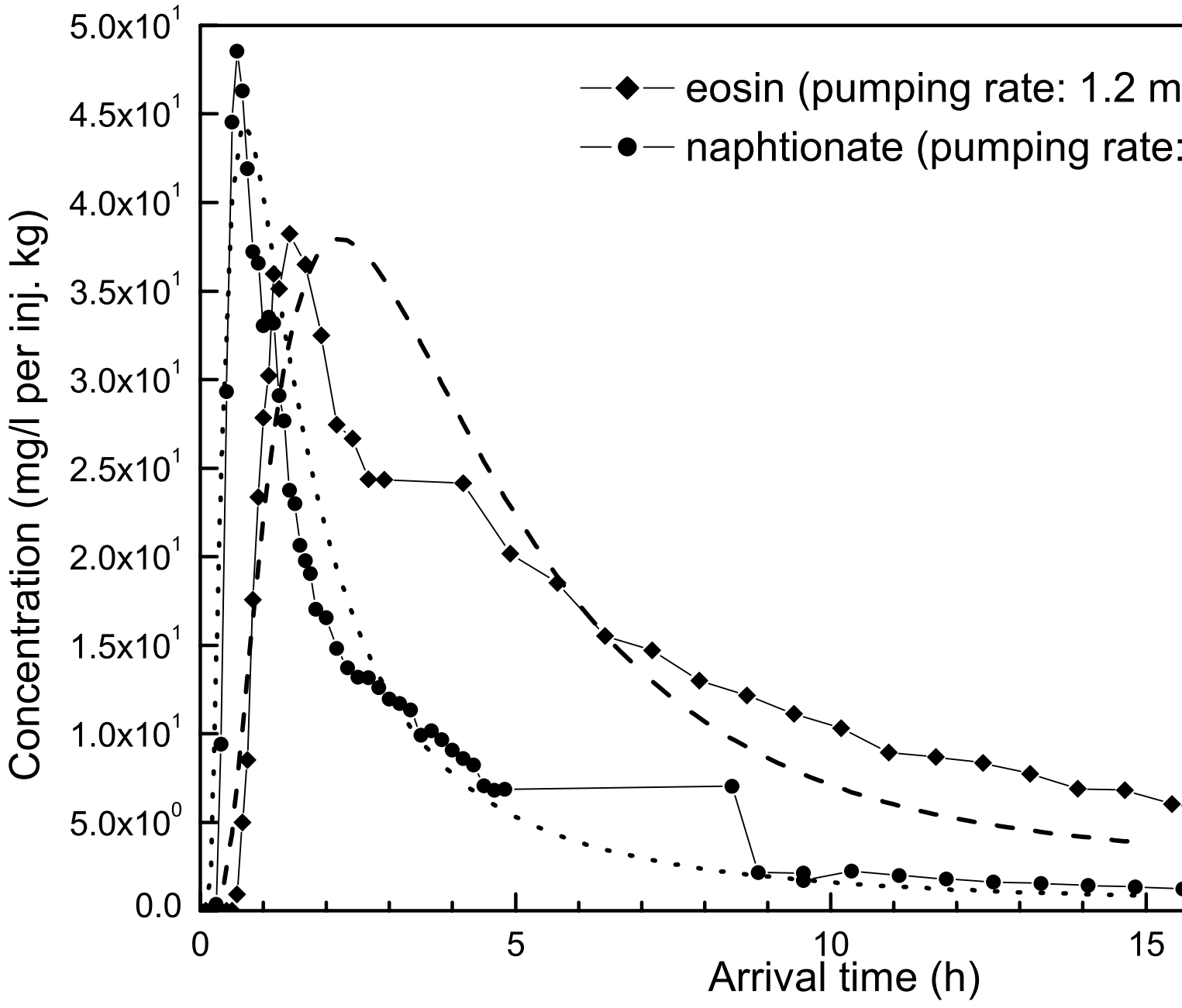
5.0x10^1
4.5x10^1
4.0x10^1
3.5x10^1
3.0x10^1
2.5x10^1
2.0x10^1
1.5x10^1
1.0x10^1
5.0x10^0
0.0
Concentration (mg/l per inj. kg)
0
5
10
15
Arrival time (h)
eosin (pumping rate: 1.2 m
naphtionate (pumping rate:

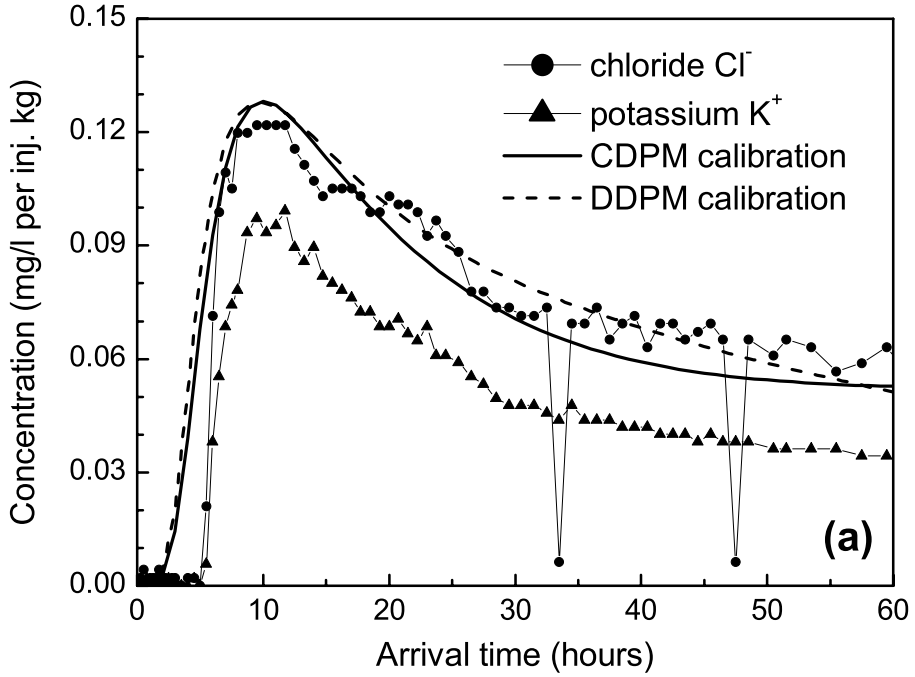
chloride Cl-
potassium K+
CDPM calibration
DDPM calibration
(a)
Concentration (mg/l per inj. kg)
Arrival time (hours)
0.00
0.03
0.06
0.09
0.12
0.15
0
10
20
30
40
50
60

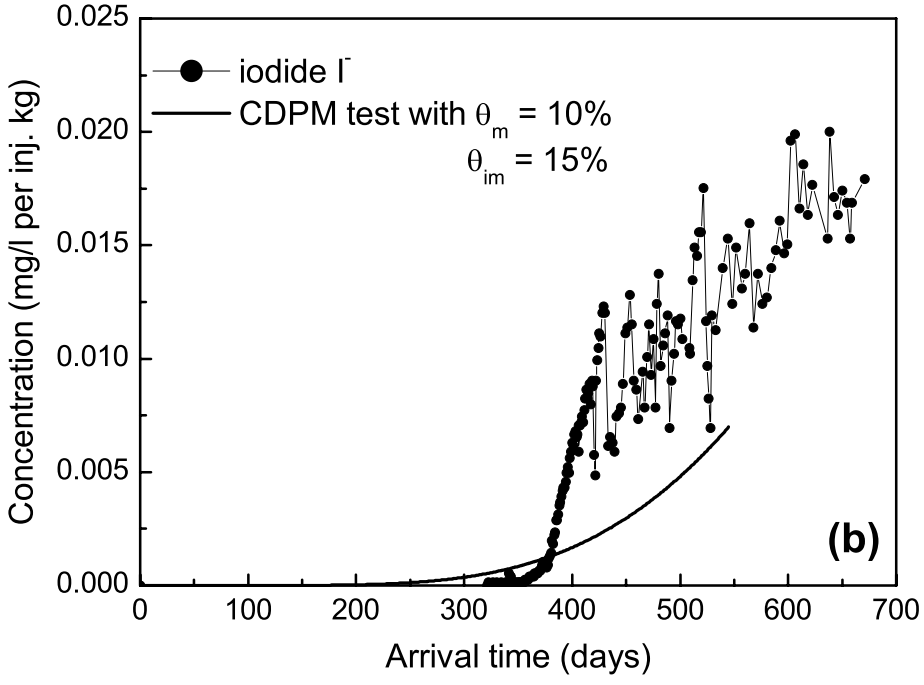
iodide I-
CDPM test with θm = 10%
θim = 15%
(b)
Concentration (mg/l per inj. kg)
Arrival time (days)
0.000
0.005
0.010
0.015
0.020
0.025
0
100
200
300
400
500
600
700